

Effect of interfacial charge on polarization switching of lead zirconate titanate particles in lead zirconate titanate/polyurethane composites

C. K. Wong^{a)}

Department of Applied Physics, The Hong Kong Polytechnic University, Hong Kong, People's Republic of China

Y. W. Wong and F. G. Shin

Department of Applied Physics, Materials Research Center and Center for Smart Materials, The Hong Kong Polytechnic University, Hong Kong, People's Republic of China

(Received 22 April 2002; accepted for publication 15 July 2002)

A simple model has been developed to include the effect of accumulated charge at the matrix–inclusion interface in ferroelectric 0–3 composites on the polarization reversal characteristics. This is used to illustrate a recent set of experimental results on initially polarized lead zirconate titanate (PZT)/polyurethane (PU) composites subjected to an increasing electric field in the reversed direction. Estimations based on previous models [e.g., T. Furukawa, K. Fujino, and E. Fukada, *Jpn. J. Appl. Phys.* **15**, 2119 (1976)] suggest that the local electric field in the PZT particles at switching was an order smaller than the coercive field of PZT. By introducing the effect of interfacial charge and assuming that initially the charge has a magnitude which balances the depolarization field in the polarized PZT inclusions, theoretical calculation based on this image shows that the phenomenon of PZT switching at low fields can be explained as a manifestation of the depletion of interfacial charge which can no longer stabilize the original polarization. © 2002 American Institute of Physics. [DOI: 10.1063/1.1505989]

I. INTRODUCTION

The study of ferroelectric 0–3 composites, usually involving a piezoelectric ceramic (e.g., PZT) and a polymer have attracted much research interest for many years. They have found many applications, such as piezoelectric and pyroelectric sensors and actuators. Polymers of large electrostriction as matrix material have also attracted attention in recent years, as in the lead zirconate titanate (PZT)/polyurethane (PU) composite.^{1–5} In a previous article,⁵ the induced strain of initially polarized PZT/PU composites subjected to an increasing electric field in the reversed direction had been measured. It has been reported that the PZT/PU composites with PZT volume fraction larger than 6% exhibited a switching characteristic when the applied electric field was increased to a critical value, and the critical electric fields decreased with increasing PZT volume fractions. The local electric field in the PZT particles during switching, calculated from the applied electric field in the usual manner (e.g., in Ref. 6), was nearly an order of magnitude smaller than the coercive field of PZT. We believe that this anomaly phenomenon is related to interfacial charge effects for which not much is known. An interesting example of an interfacial charge effect is recently given by Ploss *et al.*,⁷ and effects of charges in inhomogeneous ferroelectrics and their interaction with polarization have also attracted increasing research interest in recent years.^{8–10} This work attempts to understand the phenomenon of polarization switching of the PZT particles in PZT/PU at low external fields by suggesting that the compensating interfacial charge that originally stabilizes the

PZT polarization will find new equilibrium values under a reversed field, thus allowing the particle's depolarization field to switch the polarization. This switching process is investigated theoretically by a simple model and is found to be a manifestation of the conductivity of the constituent materials.

II. INTERNAL FIELDS AND COMPENSATING INTERFACIAL CHARGE IN 0–3 COMPOSITES

To understand the mechanism of polarization switching in the PZT particles of a 0–3 PZT/PU composite, we will first obtain the time development of the local electric field acting on an individual particle, given the external electric field. The calculation to follow will clarify the role of interfacial charge in influencing polarization switching.

As a first approximation, we assume that the constitutive equation for an electroactive dielectric is

$$D = P + \varepsilon E, \quad (1)$$

where D is electric displacement, P is switchable polarization, ε is permittivity, and E is electric field.

Consider the single inclusion problem of a dielectric sphere surrounded by the matrix medium of permittivity ε_m , with a uniform electric field applied along (say) the Z direction far away from the inclusion. The boundary value problem gives the following equation (see Appendix):

$$\langle D_i \rangle + 2\varepsilon_m(\langle E_i \rangle - \langle E_m \rangle) = \langle D_m \rangle + q_0, \quad (2)$$

where the angular brackets denote volume-averaged fields enclosed, which are nonzero only along the Z direction, and

^{a)}Electronic mail: wongck.a@polyu.edu.hk

$$\begin{cases} \langle D_i \rangle = \langle P_i \rangle + \varepsilon_i \langle E_i \rangle \\ \langle D_m \rangle = \langle P_m \rangle + \varepsilon_m \langle E_m \rangle \end{cases} \quad (3)$$

where the subscripts i and m denote ‘‘inclusion’’ and ‘‘matrix,’’ respectively. In Eq. (2), we have assumed both constituent materials are uniformly polarized and the homogeneously polarized sphere is covered with surface charge of density q_0 at the pole along the polarizing direction ($\theta=0$) with a distribution given by $q_0 \cos \theta$.

To allow a discussion on the time variation of this interfacial charge, we consider the conduction current densities j in the constituents:

$$\begin{cases} \langle j_i \rangle = \sigma_i \langle E_i \rangle \\ \langle j_m \rangle = \sigma_m \langle E_m \rangle \end{cases} \quad (4)$$

where σ_i and σ_m are electric conductivities for inclusion and matrix, respectively. Since the equations governing the conductivity problem are similar to those used in the dielectric problem (treated in the Appendix), we may follow the same calculation as for D and E for the single inclusion problem to obtain a relation between conduction current densities and electric fields in the constituents. The analogous result is

$$\langle j_i \rangle + 2\sigma_m(\langle E_i \rangle - \langle E_m \rangle) = \langle j_m \rangle - \partial q_0 / \partial t. \quad (5)$$

When compared to Eq. (2), the minus sign preceding the charge term on the right-hand side of Eq. (5) reflects the difference in the boundary conditions for the electric displacement and conduction current density.

The average electric field $\langle E \rangle$ in the composite may be obtained from the results of the single inclusion problem through the relation

$$\langle E \rangle = \phi \langle E_i \rangle + (1 - \phi) \langle E_m \rangle \quad (6)$$

which is valid for dilute suspension of inclusion particles.^{6,11} The symbol ϕ denotes the inclusion volume fraction.

Using Eqs. (2)–(6), we obtain, after some manipulation,

$$\begin{aligned} \frac{\partial \langle E_i \rangle}{\partial t} + \frac{\langle E_i \rangle}{\tau} \\ = \frac{3[\sigma_m \langle E \rangle + \varepsilon_m \partial \langle E \rangle / \partial t] - (1 - \phi) \partial [\langle P_i \rangle - \langle P_m \rangle] / \partial t}{\phi 3 \varepsilon_m + (1 - \phi)(\varepsilon_i + 2\varepsilon_m)}, \end{aligned} \quad (7)$$

where

$$\tau = \frac{\phi 3 \varepsilon_m + (1 - \phi)(\varepsilon_i + 2\varepsilon_m)}{\phi 3 \sigma_m + (1 - \phi)(\sigma_i + 2\sigma_m)}. \quad (8)$$

Equation (7) is a first order differential equation. For a given external field, which may be equated to $\langle E \rangle$, we may obtain $\langle E_i \rangle$ as a function of time t when the P – E relations for the individual constituents ($\langle P_i \rangle$ versus $\langle E_i \rangle$ and $\langle P_m \rangle$ versus $\langle E_m \rangle$) are known. In this work, the model of Miller *et al.*^{12,13} is used to describe P – E relations of the constituent materials, as will be explained in Sec. III.

From Eqs. (2) and (3), the surface charge density q_0 may be expressed as

$$q_0 = \langle P_i \rangle - \langle P_m \rangle + (\varepsilon_i + 2\varepsilon_m) \langle E_i \rangle - 3\varepsilon_m \langle E_m \rangle. \quad (9)$$

TABLE I. Properties of constituents for PZT/PU 0–3 composites.

	ε	σ ($\Omega^{-1} \text{ m}^{-1}$)	P_r (C/m ²)	P_s (C/m ²)	E_c^b (MV/m)
PZT	1570 ^a	5×10^{-12c}	0.35	0.4	1
PU	6.8 ^b	22×10^{-10d}			

^aReference 14.

^bReference 5.

^cReference 15.

^dReference 16.

Our subsequent calculations will only concentrate on the PZT/PU composites, therefore, all $\langle P_m \rangle$'s in Eqs. (7) and (9) should be set to zero since PU is nonferroelectric.

III. MODELING PARAMETERS AND HYSTERESIS LOOP OF PZT

Table I shows the permittivities and conductivities for the constituents used in this computation. For low electric fields, these values can be treated as constants and independent of the electric fields. In the experiment on the polarization switching in PZT/PU composites described in Ref. 5, the external applied field was set to increase at a rate of 0.27 MV/m per second. Thus, in Eq. (7), $\langle E \rangle = 0.27 t$ MV/m where t is expressed in seconds. Moreover, $\langle P_m \rangle = 0$ because PU is not ferroelectric while $\langle P_i \rangle$ is generally not a simple function of $\langle E_i \rangle$. For the inclusion phase, the change of polarization depends on a change of electric field as well as on the polarization already present. In our calculation, we assume that the PZT particles are fully polarized initially, i.e., $P_i(t=0) = -P_{r,i}$ where r denotes ‘‘remanent.’’ Thus, when the composite is acted upon by an increasing, positive electric field E , P_i will gradually increase, tracing the positive-field branch of the P_i – E_i hysteresis loop until saturation $P_{s,i}$ is reached. In the process, P_i changes sign when E_i passes the coercivity $E_{c,i}$. The model for a saturated hysteresis loop of a ferroelectric, suggested by Miller *et al.*,¹² may be adopted in this calculation:

$$P_i = \xi_i P_{s,i} \tanh \left[\frac{\xi_i E_i - E_{c,i}}{2E_{c,i}} \ln \left(\frac{1 + P_{r,i}/P_{s,i}}{1 - P_{r,i}/P_{s,i}} \right) \right]. \quad (10)$$

In this model, ξ_i takes $+1$ and -1 for increasing E_i and decreasing E_i , respectively. Since different kinds of ferroelectric materials may have different hysteresis loop shapes (corresponding to different $\partial P_i / \partial E_i$ for a given field) even though they have the same values of $P_{r,i}$, $P_{s,i}$, and $E_{c,i}$, we therefore have slightly modified Eq. (10) to include a factor $n_i \equiv n_{1,i} / n_{2,i}$ to extend the usage of Miller *et al.*'s model for a broader range of ferroelectrics, and, as a result, the hysteresis loop of PZT phase may be approximated by

$$\begin{aligned} \langle P_i \rangle = \xi_i P_{s,i} \left\{ \tanh \left[\frac{\xi_i \langle E_i \rangle - E_{c,i}}{2E_{c,i}} \right] \right. \\ \left. \times \ln \left(\frac{1 - (-P_{r,i}/P_{s,i})^{n_{2,i}/n_{1,i}}}{1 + (-P_{r,i}/P_{s,i})^{n_{2,i}/n_{1,i}}} \right) \right\}^{n_{1,i}/n_{2,i}}, \end{aligned} \quad (11)$$

with $n_{1,i}/n_{2,i} = 5/11$ (Fig. 1). In general, it is found that odd-numbered n_1 and n_2 with n_1/n_2 ranging from 1/3 to 1 will give results close to hysteresis loops of realistic materials.

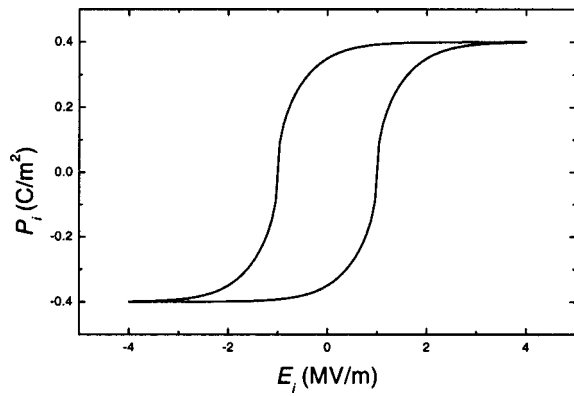


FIG. 1. Adopted P - E hysteresis loop of PZT [Eq. (11) with $n_{1,i}/n_{2,i} = 5/11$] for model calculation.

Values of $P_{r,i}$, $P_{s,i}$, and $E_{c,i}$ used in our calculation are shown in Table I. When Eq. (11) is substituted into Eq. (7), the relation $\partial\langle P_i \rangle / \partial t = [\partial\langle P_i \rangle / \partial\langle E_i \rangle][\partial\langle E_i \rangle / \partial t]$ should be employed. Concerning the initial condition of internal fields, our theoretical calculations assume electric fields in the constituents are both initially zero. Therefore, from Eq. (9)

$$q_0(t=0) = \langle P_i(t=0) \rangle = -P_{r,i}. \quad (12)$$

Equation (12) gives the sign and magnitude of the charge density $q_0 \cos \theta$ of the free surface charge accumulated at the matrix-inclusion interface at $t=0$ which completely balances the depolarization field inside a fully polarized inclusion particle.

IV. RESULTS AND DISCUSSION

A previous article⁵ reported the experiment as follows: The PZT/PU composite samples were first polarized, then an increasing external electric field was applied in the reversed direction (opposite to the remanent polarization in the PZT particles). The rate of increase of the field was set at 0.27 MV/m per second. By monitoring the time development of the electrostrictive strain of the thickness of the composite, the critical electric field which corresponded to polarization reversal in the PZT phase was obtained since the induced strain changed sign when the polarization of PZT switched direction. Wong *et al.*⁵ also reported that pure PZT experienced polarization reversal at about 1 MV/m (i.e., coercive field $E_c \approx 1$ MV/m). Without considering the effect of interfacial charge, the electric field in the inclusion phase at switching may be estimated from the magnitude of the applied electric field (Fig. 2) together with the permittivity value of the composite⁵ and those of the constituent materials:^{6,11}

$$\langle E_i \rangle = \frac{1}{\phi} \frac{\epsilon - \epsilon_m}{\epsilon_i - \epsilon_m} \langle E \rangle. \quad (13)$$

Calculations from Eq. (13) have suggested that the $\langle E_i \rangle$ value at polarization switching is about 0.1 MV/m for all the composite samples investigated (PZT volume fraction from 6% to 38%). This is about an order of magnitude smaller than the coercive field of PZT, which is difficult to understand.

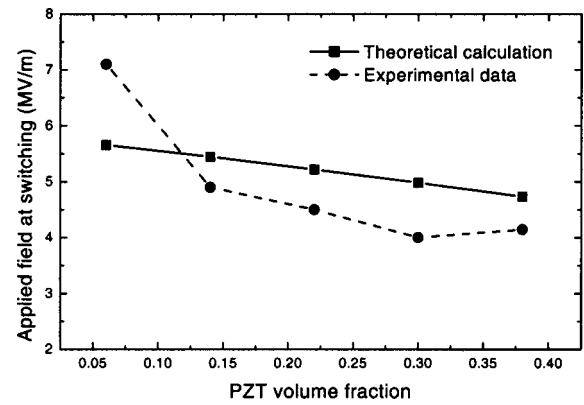


FIG. 2. Applied electric field at polarization reversal vs the volume fraction of inclusion phase.

To solve the discrepancy, we employ the model developed in Sec. III, which has included the effect of accumulated charge at the matrix-inclusion interface in the ferroelectric 0-3 composite, to study polarization reversal characteristics. In Fig. 2, the experimental result of the switching electric fields (the external electric field at polarization reversal) for the PZT/PU composites of different inclusion volume fractions are to be compared with the theoretical predictions obtained by solving Eq. (7). The switching mechanism is schematically shown in Fig. 3. Figure 3(a) illustrates the initial residence of charge around an inclusion within the composite, where the polarization of the inclusion phase (which is taken as the remanent polarization) is completely balanced by the free surface charge [Eq. (12)] at the matrix-inclusion interface. When an electric field opposite to the inclusion polarization is applied to the composite sample, the polarization will no longer be fully balanced by charge [Fig. 3(b)], as some interfacial charges are removed by the electric field because the constituent materials have finite conductivities. As a result, the uncompensated polarization charge gives rise to a depolarization field pointing in the same direction as the applied field. The polarization of the inclusion phase will then be reduced and eventually switched to the opposite direction when the electric field in the inclusion reaches coercivity.

This process becomes apparent when Eq. (7) is solved with supplementary and initial conditions as explained in Sec. III. Taking $\phi = 0.06$ and 0.22 as examples, Fig. 4 shows the development of the electric field in the inclusion as the electric field applied on the composite is increased. Since PZT has a coercive field of about 1 MV/m, the polarization of the inclusion phase will switch when the internal field $\langle E_i \rangle$ reaches 1 MV/m. We can therefore find the applied electric field value $\langle E \rangle$ from Fig. 4 corresponding to the coercive field required to switch the polarization of the PZT and the results are shown in Fig. 2. A remark should be made which relates to the shape of the curve $\langle E_i \rangle$ vs $\langle E \rangle$. The shape of this curve substantially depends on the adopted hysteresis loop for PZT, but, in contrast, it will not affect the location of the critical external electric field (at PZT switching) significantly. We have attempted to use other loop shapes for PZT to verify the similarity and consistency of the

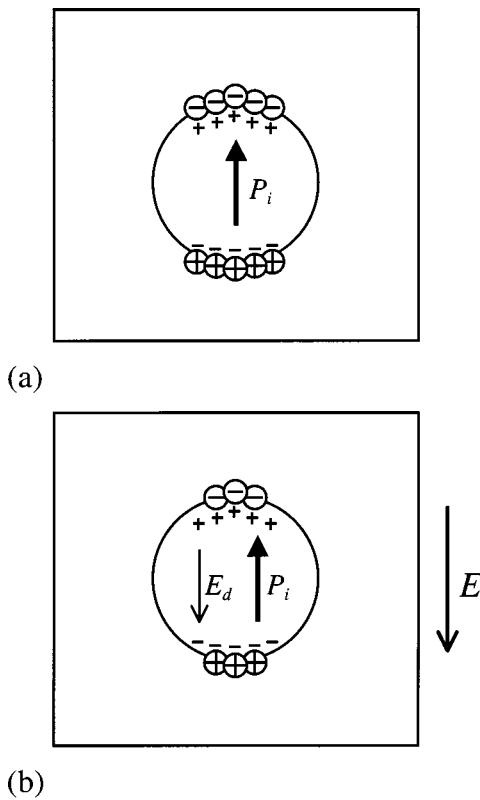


FIG. 3. Schematic diagrams of interfacial charge around an inclusion particle within a composite sample, with symbols \oplus and \ominus denoting free charges, and symbols $+$ and $-$ denoting bound polarization charges. (a) Polarized sphere is fully compensated by free charges, and (b) depolarization field E_d is induced because of depletion of interfacial charge when the composite is subjected to an applied electric field E .

critical switching field values. The critical electric fields of the PZT/PU composites of different PZT volume fractions have been shown in Fig. 2. Both the experimental and our calculated critical fields decrease with increasing PZT volume fraction. Apart from the sample with 6% PZT volume fraction, the magnitude as well as the decreasing trend of the predicted critical field is in fairly good agreement with the measured values.

Taking the coercive field of PZT as 1 MV/m, estimations based on previous models [Eq. (13)] will give the critical

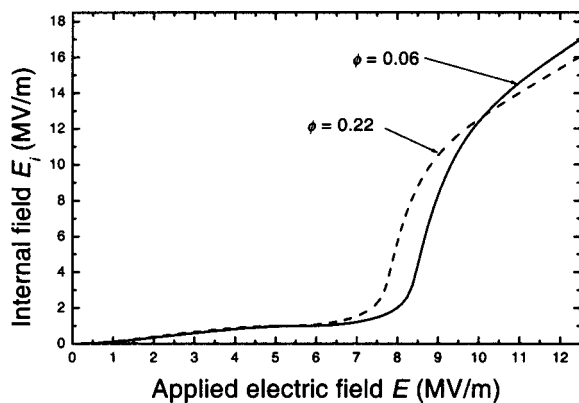


FIG. 4. Theoretical results of the internal field $\langle E_i \rangle$ vs the applied electric field $\langle E \rangle$ for $\phi = 0.06$ and $\phi = 0.22$.

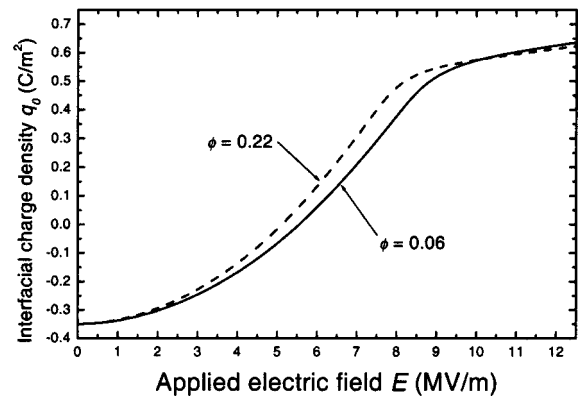


FIG. 5. Theoretical results of the surface charge density q_0 vs the applied electric field $\langle E \rangle$ for $\phi = 0.06$ and $\phi = 0.22$.

electric fields at switching from 100 to 25 MV/m for inclusion volume fractions from 0.06 to 0.38. These values are about an order of magnitude higher than our model predictions. Our model [Eq. (7)] takes interfacial charge into account and gives the critical electric fields at switching from 5.66 to 4.73 MV/m for inclusion volume fractions from 0.06 to 0.38, which are in fairly good agreement with experimental data as shown in Fig. 2. This confirms that the consideration of the interfacial charge effect in the polarization reversal phenomenon is essential.

Figure 5 shows the interfacial charge density q_0 versus the applied electric field for $\phi = 0.06$ and 0.22, respectively [calculated from Eq. (9)]. It clearly demonstrates that, as the applied electric field increases, the charge density q_0 increases (becoming more positive) and eventually changes sign. This is consistent with the image shown in Fig. 3.

V. CONCLUSIONS

Based on a simple model that includes the effect of interfacial charge on polarization switching of PZT particles in PZT/PU composites, the phenomenon that the PZT polarization is able to reverse at electric fields much lesser than coercivity can be understood. This demonstrates that considerations of interfacial charge are essential to understanding the behavior of ferroelectric composites. Convenient mathematical functions (hyperbolic tangents) have been adopted for the $P-E$ relationship of PZT. The calculated switching fields for the composites are compared with the experimental values. The experimental results reveal that the switching field decreases with increasing PZT volume fraction and this trend is broadly predicted by the present model. The formulation of this model can be readily applied to other studies. By modifying Eq. (10) to capture the major characteristics of a real $P-E$ curve for a ferroelectric material, this model may be used to simulate the electrical response of other composites with small inclusion volume fraction. However, in situations where it is necessary to consider a more general $P-E$ relationship of the constituents than the saturated hysteresis loop, e.g., in the poling of composites, modeling of general ferroelectric responses such as provided by Miller *et al.*¹³ may be employed.

ACKNOWLEDGMENT

This work was supported by the Center for Smart Materials of the Hong Kong Polytechnic University Research Grant.

APPENDIX

Consider a dielectric sphere of radius a with permittivity ε_i subjected to a uniform electric field $\langle E_m \rangle$ in the Z direction far away from the sphere. The sphere is surrounded by a medium with permittivity ε_m . The problem is to solve Laplace equations with azimuthal symmetry:

$$\nabla^2 \varphi_i = 0, \quad (\text{A1})$$

$$\nabla^2 \varphi_m = 0, \quad (\text{A2})$$

where σ_i and σ_m are the electric potential inside and outside the sphere, respectively.

With the condition that σ_i must not have a singularity at the center of sphere ($r=0$), and the boundary condition at infinity:

$$(\varphi_m)_{r \rightarrow \infty} = -\langle E_m \rangle z = -\langle E_m \rangle r \cos \theta \quad (\text{A3})$$

solutions of Eqs. (A1) and (A2) give

$$\varphi_i = \sum_{l=0}^{\infty} A_l r^l P_l(\cos \theta), \quad (\text{A4})$$

$$\varphi_m = -\langle E_m \rangle r \cos \theta + \sum_{l=0}^{\infty} C_l r^{-(l+1)} P_l(\cos \theta), \quad (\text{A5})$$

where $P_l(\cos \theta)$ are the Legendre polynomials.

The boundary condition of the tangential component of electric field is

$$-\frac{1}{r} \frac{\partial \varphi_i}{\partial \theta} \Big|_{r=a} = -\frac{1}{r} \frac{\partial \varphi_m}{\partial \theta} \Big|_{r=a}, \quad (\text{A6})$$

and the boundary condition of the normal component of electric displacement is

$$\begin{aligned} -\varepsilon_i \frac{\partial \varphi_i}{\partial r} + \langle P_i \rangle \cos \theta \Big|_{r=a} \\ = -\varepsilon_m \frac{\partial \varphi_m}{\partial r} + \langle P_m \rangle \cos \theta \Big|_{r=a} + q_0 \cos \theta. \end{aligned} \quad (\text{A7})$$

We assume that the polarization terms P_i and P_m , denoted by the average in the respective phases, are uniform in each of the spherical inclusion and continuous matrix regions, and that the spherical inclusion is covered by charges with a surface charge density $q = q_0 \cos \theta$. These assumptions make Eqs. (A1) and (A2) plausible.

Applying the boundary conditions to Eqs. (A4) and (A5),

$$\begin{aligned} \left[-A_1 - \langle E_m \rangle + \frac{C_1}{a^3} \right] a \sin \theta + \sum_{l=2}^{\infty} \left(A_l - \frac{C_l}{a^{2l+1}} \right) \\ \times a^l \frac{\partial P_l(\cos \theta)}{\partial \theta} = 0, \end{aligned} \quad (\text{A8})$$

$$\begin{aligned} \left[\left(\frac{\varepsilon_i}{\varepsilon_m} \right) A_1 + \langle E_m \rangle + 2 \frac{C_1}{a^3} - \frac{\langle P_i \rangle - \langle P_m \rangle - q_0}{\varepsilon_m} \right] \cos \theta \\ + \sum_{l=2}^{\infty} \left[\left(\frac{\varepsilon_i}{\varepsilon_m} \right) l A_l + (l+1) \frac{C_l}{a^{2l+1}} \right] a^{l-1} P_l(\cos \theta) = 0, \end{aligned} \quad (\text{A9})$$

Equations (A8) and (A9) can be satisfied simultaneously only when $A_l = C_l = 0$ for $l \geq 2$, therefore, they become

$$A_1 - \frac{C_1}{a^3} = -\langle E_m \rangle, \quad (\text{A10})$$

$$\left(\frac{\varepsilon_i}{\varepsilon_m} \right) A_1 + 2 \frac{C_1}{a^3} = -\langle E_m \rangle + \frac{\langle P_i \rangle - \langle P_m \rangle - q_0}{\varepsilon_m}. \quad (\text{A11})$$

Eliminating C_1 from Eqs. (A10) and (A11) and then substituting A_1 into Eq. (A4), the electric field inside the sphere (evaluated from the electric potential) is

$$\langle E_i \rangle = \frac{2\varepsilon_m \langle E_m \rangle - \langle P_i \rangle + (\varepsilon_m \langle E_m \rangle + \langle P_m \rangle) + q_0}{\varepsilon_i + 2\varepsilon_m}. \quad (\text{A12})$$

We can finally rewrite this equation in terms of the electric displacements $\langle D_i \rangle = \varepsilon_i \langle E_i \rangle + \langle P_i \rangle$ and $\langle D_m \rangle = \varepsilon_m \langle E_m \rangle + \langle P_m \rangle$ to obtain

$$\langle D_i \rangle + 2\varepsilon_m (\langle E_i \rangle - \langle E_m \rangle) = \langle D_m \rangle + q_0. \quad (\text{A13})$$

- ¹W. K. Sakamoto, S. Kagesawa, D. H. Kanda, and D. K. Das-Gupta, *J. Mater. Sci.* **33**, 3325 (1998).
- ²W. K. Sakamoto, S. Shibatta-Kagesawa, D. H. F. Kanda, S. H. Fernandes, E. Longo, and G. O. Chierice, *Phys. Status Solidi A* **172**, 265 (1999).
- ³W. K. Sakamoto, S. T. Shibatta-Kagesawa, and W. L. B. Melo, *Sens. Actuators A* **77**, 28 (1999).
- ⁴Y. W. Wong, L. S. Tai, C. X. Liu, and F. G. Shin, *Ferroelectrics* **264**, 57 (2001).
- ⁵Y. W. Wong, C. X. Liu, L. S. Tai, and F. G. Shin, *Proc. SPIE* **4329**, 516 (2001).
- ⁶T. Furukawa, K. Fujino, and E. Fukada, *Jpn. J. Appl. Phys., Part 1* **15**, 2119 (1976).
- ⁷B. Ploss, B. Ploss, F. G. Shin, H. L. W. Chan, and C. L. Choy, *Proc. IEEE* **1**, 301 (2002).
- ⁸G. M. Sessler, *J. Electrostat.* **51**, 137 (2001).
- ⁹G. Damamme, C. Le Gressus, and A. S. De Reggi, *IEEE Trans. Dielectr. Electr. Insul.* **4**, 558 (1997).
- ¹⁰D. Rollik, S. Bauer, and R. Gerhard-Mulhaupt, *J. Appl. Phys.* **85**, 3282 (1999).
- ¹¹C. K. Wong, Y. M. Poon, and F. G. Shin, *J. Appl. Phys.* **90**, 4690 (2001).
- ¹²S. L. Miller, R. D. Nasby, J. R. Schwank, M. S. Rodgers, and P. V. Dressendorfer, *J. Appl. Phys.* **68**, 6463 (1990).
- ¹³S. L. Miller, J. R. Schwank, R. D. Nasby, and M. S. Rodgers, *J. Appl. Phys.* **70**, 2849 (1991).
- ¹⁴L. S. Tai, M. Phil. Thesis, The Hong Kong Polytechnic University, 2001.
- ¹⁵H. L. W. Chan, Y. Chen, and C. L. Choy, *Integr. Ferroelectr.* **9**, 207 (1995).
- ¹⁶J. E. Mark, *Polymer Data Handbook* (Oxford, New York, 1999), p. 874.